International Journal of Chemical Studies

P-ISSN: 2349–8528
E-ISSN: 2321–4902
www.chemijournal.com
IJCS 2023; 11(3): 37-45

Received: 20-01-2023
Accepted: 27-02-2023

Uddhav M Jadhav
Department of Chemistry, Poojya Sane Guruji Vidya Prasarak Mandal's Sajan Isan Patil Arts, Girdhar Barku Patel Science and Shahada Taluka Kharedi Vikri Sangh Commerce College, Khetia Road Shahada, Nandurbar, Maharashtra, India

Corresponding Author:
Department of Chemistry, Poojya Sane Guruji Vidya Prasarak Mandal's Sajan Isan Patil Arts, Girdhar Barku Patel Science and Shahada Taluka Kharedi Vikri Sangh Commerce College, Khetia Road Shahada, Nandurbar, Maharashtra, India

Study of several rare earth ions and transition metals in their luminescent transition states

Uddhav M Jadhav

Abstract
This work examines in depth the luminescence transition states of several rare earth ions (Ce^{3+}, $Pr^{3+,}$ Nd^{3+}, $Sm^{3+,}$ Sm^{2+}, Eu^{2+}, Eu^{3+}, Gd^{3+}, Tb^{3+}, Dy^{3+}, Er^{3+}, Tm^{3+}, Yb^{3+}) as well as Mn^{2+}, Cr^{3+}, and Cu^{+}, which are transition metal ions. When rare earth and transition metal ions are added, luminous materials will be excited and will emit light at various energy levels. Luminescence transition states of rare earth ions and transition metal ions are studied in detail.

Keywords: luminescence, rare earth ions, transition metal ions, spectroscopy

1. Introduction
The phenomenon emission of light by certain kinds of substance on absorbing various energies without heat generation is called luminescence It is in comparison to light emitted from incandescent bodies, including burning wood or coal, molten iron, and wire heated with the aid of an electric current. These are all incandescent resources of light and convert simplest five% of power into visible light.

Luminescence is closely related to spectroscopy, that is examine of the overall laws of absorption and emission of radiation with the matter [1]. Since the dawn of time, humans have been affected by luminescent phenomena [2]. Examples of naturally occurring luminescence include the aurora borealis, glow worms, luminescent wood, decaying fish, and flesh. The existence of luminous organisms which includes bacteria in the sea and in decaying natural count, glow worms and fireflies have mystified and thrilled guy due to the fact time immemorial. A systematic scientific study of the subject of luminescence is of recent origin. Zechi made a significant contribution to the understanding of photoluminescence in 1652. It is the emission of light that continues after the excitation agent is taken away. Additionally, he used experiments to demonstrate that the colour of the phosphorescence light in a material is independent of the colour of the stimulating light and to provide a clear distinction between the phenomena and scattering. 200 years or so later [3]. In 1852 English Physicist G.C. Stokes identified this phenomenon and formulated his regulation of luminescence now it is referred to as Stoke's law, which states that, which states that the wavelength of the emitted light is greater than that of the exciting radiation which accompanies photoluminescence. E. Bequerel made a distinction between two types of phosphorescence or afterglow in 1867, which had been attributed to monomolecular and bimolecular decay mechanisms, respectively. German physicist Eilhardt Wiedemann coined the term "Luminescence" in 1888, which unifies fluorescence and phosphorescence. This word's root is the Latin word "lumen," which denotes light [3]. In 1930, first phosphor coated fluorescent lamp was invented with efficiency of 20% but performance isn't always successful to conquer the problem of aid crunch but it opened new era of research for excellent phosphor within the discipline of luminescence. Luminescence is an interdisciplinary science and it's far studied in several fields like physics, chemistry, material science, geology, environmental science, forensic science, medical science, biological science, engineering technology, palaeontology and many others.

Over the past few decades, there have been significant quality and quantity changes in investigations of luminescence phenomena. It is clear that developments in this area have had a significant global impact on the development of science and technology over the past 60 years.

Recent studies on luminescence use inorganic and organic materials that have been stimulated by rare earth ions and transition metal ions, which is characterised by considerable interaction between many fields of luminescence and other aspects of solid-state physics. There have been both theoretical and experimental techniques.

2. Luminescence in phosphors

Activator ions are integrated into a host lattice, which is the basic building block of a phosphor. These ions create the energy levels that lead to luminescence. In general, there are two types of activator ions that may be distinguished: the first type has emission electronic states that interact weakly with the host lattice, and the second kind has strong interactions.

Since their inner 4f shells are where luminescence transitions occur [4], which are substantially insulated by outside electrons, the bulk of trivalent rare earth ions fall into the first class.

The elements majority in the IVB, VB, and VIB groups (such as Ti^{4+},V^{5+} and Mo^{6+}) are part of the second class, represented by a variety of ions, including (i) the transition metal elements, where the luminescent transitions occur between the d-d and d-s states, (ii) the s^2 ions, which have filled s shells in their ground states [4], and (iii) the transition metal Tm^{3+}, Tb^{3+}, and Eu^{3+} are examples of weakly interacting rare earth activators that exhibit this so-called characteristic luminescence [5] with narrow emission lines. Almost completely independent of the host lattice is how these lines are positioned spectrally. Broad emission bands are visible in the strongly interacting activators, though. Another result of the rare earth ions is that the activators' actual mutual interaction is usually negligible. In compared to the concentrations used for the second class of activators, a higher concentration of rare earth ions can usually be introduced without discernible concentration quenching [5].

The 4f-4f transitions of RE ions are line-shaped because the filled $5s^25p^6$ sub shells shelter the 4f orbitals, and the energy of the levels involved in transition are well defined and do not vary in different hosts [6]. the selection criteria for parity forbidden 4f-4f transitions are developed based on a number of presumptions that are not always confirmed in practice. Even while the 4f- 5d transition of RE ions is parity allowed and efficient, the symmetries of the crystal lattice sites where RE ions reside, for instance, have some influence on the parity of 4f wave functions and are not entirely pure. The d-d parity forbidden transitions of TM ions are significantly influenced by the host lattice phonon [7], resulting in parity permitted transitions. The coordination environment can be changed to control both the broadband-shaped 4f-5d transitions of RE ions and the d-d transitions of TM ions [7, 8].

A luminous material's ability to transport energy has a significant impact on its phosphor characteristics. One possibility for the absorbed energy can migrate to the crystal surface or to lattice defects, where it will be destroyed by radiation less transition. The quantum efficiency of phosphor declines as a result. In response to excitation, the radiation either undergoes absorption by included impurity ions or forms electron-hole pairs in the host lattice that transfer energy to the activator ions [9]. For the mercury radiations with a wavelength of 254 nm, the majority of applied lamp phosphors undergo the impurity absorption process. Direct activators or sensitizer effects are produced by the impurity ions. In the latter scenario, an energy transfer technique other than radiation is used to transfer energy to the activator ion results in non-radiation less transition.

Rare-earth elements have distinct outer electron configurations that include two vacant shells, and as a result, they take up extremely specialized places in solid-state physics and chemistry. Hence, rare-earth ions are used as activators in a wide range of luminescent materials and systems [10, 11]. Rare-earth ion-activated materials, such as phosphors [12-14], have outstanding quantum efficiency in the visual region [15]. Doped rare-earth ion materials have drawn a lot of interest in recent years for their luminescence study because of their chemical stability in natural environments [16]. Rare-earth ions often have weaker oscillators than transition metal ions, which allows them to absorb more of the input energy. The lanthanide elements Ce^{3+}, Pr^{3+}, Sm^{3+}, Eu^{3+}, Tb^{3+}, and Dy^{3+} are among the 15 that could be utilised in LEDs and other display technology. Nd^{3+}, HO^{3+}, Er^{3+}, Tm^{3+}, and Yb^{3+}, among other elements, exhibit nearly visible-light behavior [17]. The visible to NIR emission bands are apparent in NIR emission spectra [18-21].

The luminous transition states of several rare earth ions and transition metal ions are thoroughly covered in this study.

3. Luminescent transition states of some rare earth ions

3.1 Ce^{3+}

Cerium-doped materials frequently show strong broad-band PL. The host lattice has a significant impact on luminescence throughout the electromagnetic spectrum, from the ultraviolet to the red [22].

Despite having the lowest 4f–5d transition energy of any lanthanide ion, Ce^{3+} functions as a dependable light-emitting state due to the enormous energy gap between the 5d level and the nearest level, ^{2}F5/2.The two emission peaks that the Ce^{3+} triggered phosphors typically exhibit are caused by their two termination levels, ^{2}F5/2 and ^{2}F7/2 [23, 24]. Ce^{3+} luminescence's is highly dependent on the host lattice [3, 25].

There are only two $4f^1$ energy levels produced by the [Xe] $4f^1$ configuration of the Ce^{3+} ion, the ^{2}F5/2 and ^{2}F7/2states. The distance between these energies is about 2000 cm^{-1}. The $4f^05d^1$ bands are present at higher energies. With an average total splitting of roughly 10,000 cm^{-1}, the crystal field splits the $5d^1$ state into a number of components. Broad bands in the spectrum are visible for the 4f–5d transitions, which are totally allowed [26].

The emission occurs when the $5d^1$ state changes from its ground state to its lowest crystal field component. The emission band has two maxima because of the spin orbit splitting of the ground state. The ^{2}D3/2 and ^{2}D5/2 spin orbit split states in the free Ce^{3+}, 5d configuration are located at 49,700 and 52,100 cm^{-1} above the ground state of Ce^{3+} (^{2}F5/2) in the 5d configuration [27].

The host lattice has a significant impact on the energy of these bands [28]. The 4f to 5d transitions of the rare-earth ion Ce^{3+} are well known for producing a broad band emission in the UV to visible spectrum [29].

The asymmetric emission band in Ce3+ is caused by transitions from the lowest lying excited state $5d^1$ to the $^2F_{5/2}$ and $^2F_{7/2}$ ground states of Ce^{3+}.[i] [30] Due to the fact that the crystal field around the Ce^{3+} ions has a considerable impact on the 5d levels in Ce^{3+}, Ce^{3+} emission often exhibits high site dependence. When Ce^{3+} ions are doped into a host with many cation sites, Ce^{3+} emissions typically happen [28]. The crystal field further divides the ^{2}D3/2 and ^{2}D5/2 states, lowering the average energy of the 5d configuration [3].

Since both the emission and the absorption of Ce^{3+} result from permitted transitions, this emission also has the additional feature of having a rapid decay time (of the order of few ns).

In situations where rapid decay times are needed, Ce^{3+} phosphors are helpful (e.g. in time of flight cameras and scintillators) [31]. Ce^{3+} - Ce^{3+} transfer, followed by delivery to the killing site, causes the luminescence of Ce^{3+} concentration to be essentially quenched at 5% [32]. Ce typically exhibits a high quenching temperature in phosphates, borates, and silicates. Ce^{3+} can be employed as a sensitizer for rare earth [33] such as Tm^{3+}, Sm^{3+}, Dy^{3+}, Tb^{3+}, Nd^{3+}, Gd^{3+}, and Pr^{3+}because it exhibits significant absorption in a variety of hosts and emission that matches 4f levels of other RE impurities. Additionally, Ce^{3+}has the ability to sensitize the luminescence in hosts that include transition metal activators like Mn [31].

While the emission in (Y, Ce)3Al5O12 is in the form of a very broad spectrum from 500 nm to well beyond 700 nm, with a maximum at about 550 nm, and in sulphides like CaS and Y2O2S, it is in the green-red area [34]. The emission in (Y, Ce) PO4 is between 324 and 350 nm. Normal emission occurs in the blue region. When the crystal field is extremely strong and the centre of the 5d level is at relatively low energies (high Nephelauxetic effect), emission at longer wavelengths is obtained [31].

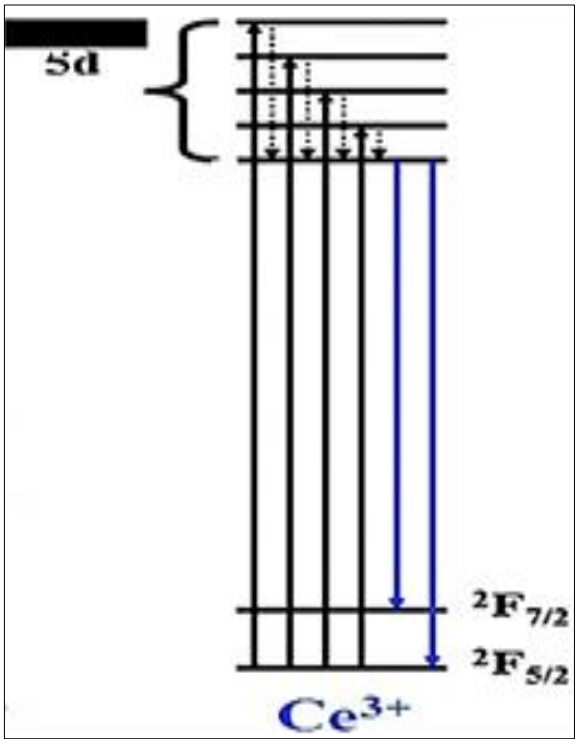

Fig 1: Energy level diagram of Ce^{3+}

3.2 Dy^{3+}

The main Dy^{3+} emission lines in the visible area are $^4F9/2$ - $^6H15/2$ (470–500 nm) and $^4F9/2$ - $^6H13/2$ (570–580 nm), respectively. The relative intensities of the two bands are influenced by local symmetry. When the ratio of blue to green emission is appropriate, as shown in Figure 2, Dy^{3+} can create white emission. In Dy^{3+} luminescence, this capability has generated some interest. Whereas Dy^{3+}, CT's state, and the 5d levels are all placed above 50000 cm^{-1} [35].

UV cannot effectively excite Dy^{3+} but Ce^{3+}, Bi^{3+}, Gd^{3+}, Pb^{2+}, and vanadate [ii], [iii] [36-37] ions can all sensitize Dy^{3+}. Dy^{3+} doped luminescent phosphors are a useful lamp phosphor. Dy doped phosphors can also be used for thermoluminescence-based ionising radiation dosimetry [38]. For personnel monitoring, phosphors like CaSO4: Dy, CaF2: Dy, and MgB4O7: Dy are used in thermo luminescence dosimetry [39].

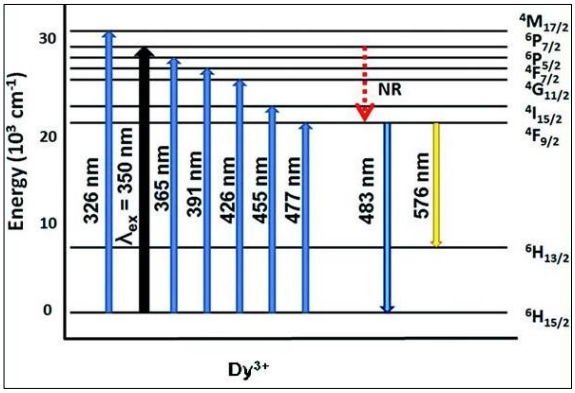

Fig 2: Energy level diagram of Dy^{3+}

3.3 Eu^{3+}

Eu^{3+} emission is typically seen via $^5D0$ -^7Fj transitions, with Eu^{3+} excitation typically occurring through the CT band or from energy transfer and host lattice absorption [40]. Figure 3 shows three transitions that are particularly significant: $^5D0$ - $^7F0$ (about 570 nm), $^5D0$ - $^7F1$ (around 595 nm), and $^5D0$ - $^7F2$ (around 610 nm). Although the first transition is strictly prohibited, it can be seen in some hosts with a respectable amount of intensity. As a magnetic dipole, the $^5D0$ - $^7F1$ transition is permitted but not as an electric dipole [41]. Only during this transition does Eu^{3+} occupy a location that also happens to be a symmetry center. When the Eu^{3+} ion is situated at a location lacking inversion symmetry, the transitions corresponding to even values of j (other than 0) are electric dipole allowed and red emission can be observed [27, 42]. Luminescence Commercial red phosphors like YVO4, Y2O3, and Y2O2S all contain Eu^{3+} ions that occupy the site without inversion symmetry. The $^5D0$ to $^7F1$ transition can also be seen in the presence of a magnetic dipole [41]. Additionally, each line corresponding to these transitions divided into the number of components that the local symmetry determined [40, 43]. The spectra are also susceptible to chemical bonding and different cation sizes [44].

In addition to $^5D0$, emission is also visible at $^5D2$ (blue) and $^5D1$ (green) levels. This emission is reduced in intensity at higher temperatures as a result of thermally induced excitations in the CT band and cross relaxations at the $^5D0$ level. Higher concentrations of europium (> 5 mol %) can also cause the cross relaxation to happen. Commercial red phosphors like YVO4, Y2O3, and Y2O2S have luminescence Eu^{3+} ions that occupy the site without inversion symmetry.

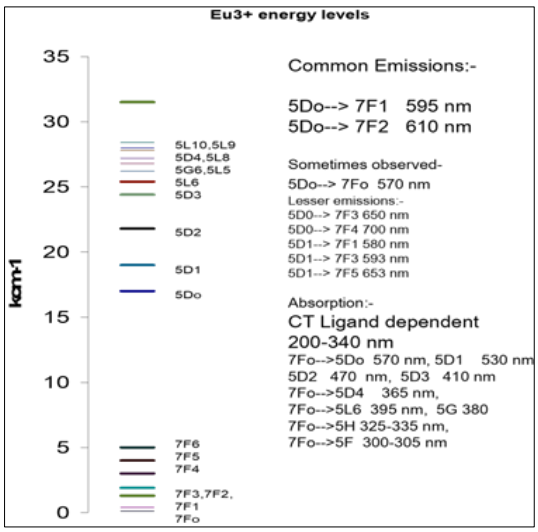

Fig 3: Energy levels of Eu^{3+}

3.4 Pr^{3+}

Pr^{3+} luminescence may be caused by a variety of multiplets, including the following: Observed transitions include those at 515 nm caused by the (^{3}P0 - ^{3}H4) transition, 670 nm caused by the (^{3}P0.^{3}F2) transition, 770 nm caused by the (^{3}P0- 3F4) transition, 630 nm caused by the (^{1}D2 3H4) transition, 419 nm caused by the (^{1}S0 - ^{1}I6) transition, and ultraviolet (5d - 4f) transitions. The host lattices affect how intense the peaks are relative to one another. In Y2O2S:Pr^{3+}, ^{3}P0 - 3F2 causes the Pr^{3+} doped ZnO-Gd2O3/GdF3-BaO-P2O3iv [19] to produce light at 670 nm.

The CaSnO3 sample doped with Pr^{3+} produced the primary emission peak at 490 nm and the weak emission peaks at 533 and 615 nm, which are related to the transitions of ^{3}P0 - ^{3}H4, ^{3}P0 - ^{3}H5, and ^{1}D2- ^{3}H4 respectively [46].

Under deep UV stimulation, natural fluorite, anhydrite, and apatite show multiple narrow emission bands in the 225-300 nm spectral range, with the greatest peaks at 230-240 nm and 260-290 nm. Due to 4f5d -4f transitions in the Pr^{3+} luminescence center, [47] they have a narrow excitation band with a peak at 220 nm, which is characteristic of them [48]. Doped Pr^{3+} up conversion phosphors can be a great choice for solar cell applications like UV/NIR to visible converters and solid-state lighting [47].

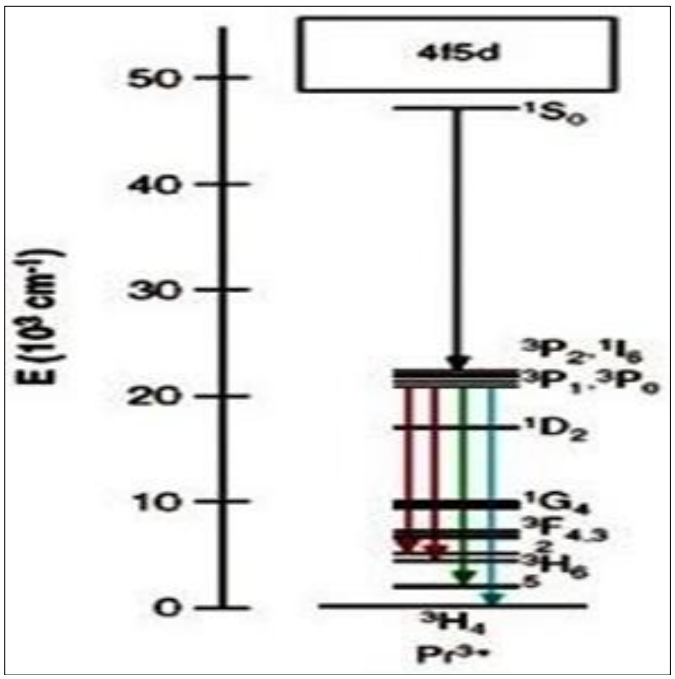

Fig 4: Energy level diagram of Pr^{3+}

3.5 Nd^{3+}

When used as an activator in the infrared region, Nd^{3+} ions produce the following transitions in Y3N5O12:Nd^{3+}, these peaks have been seen [49]. Peaks are detected between 870 and 950 nm due to the transition ^{4}F3/2 - 4I9/2, [50] related to the transitions ^{4}F3/2 - ^{4}I11/2 between1050 and 1120 nm and ^{4}F3/2 - ^{4}I13/2 between 1340 and 1440 nm. [51] Padlyak B *et al*. investigated the luminescence (emission and excitation) spectra in a variety of borate glasses with compositions containing Li2B4O7: Nd, LiCaBO3:Nd, and CaB4O7:Nd and 0.5 and 1.0 mol% Nd2O3. Only the network of studied glasses contains Nd^{3+} (^{4}F3/2, ^{4}I9/2) ions, the Nd impurity. The optical absorption and luminescence spectra of the tested glasses' Nd^{3+} centres were all found to be relevant for laser applications [52].

Phosphate-based laser glasses with a 1 mol% Nd^{3+} embedding have been explored by Samar Jana *et al*. When the glasses are excited at 585 nm, a strong emission caused by the ^{4}F3/2 ^{4}I11/2 transition at 1055 nm in the near infrared (NIR) region is seen in the glasses. Phosphate-based laser glasses have detected a range of luminescence emission for ^{4}F3/2 - 4IJ(J = 9/2, 11/2, and 13/2) transitions. Neodymium doped phosphate-based laser glasses demonstrate that the more effective laser active material for emission in the NIR region at 1055 nm is the Nd^{3+} activated luminescence [53].

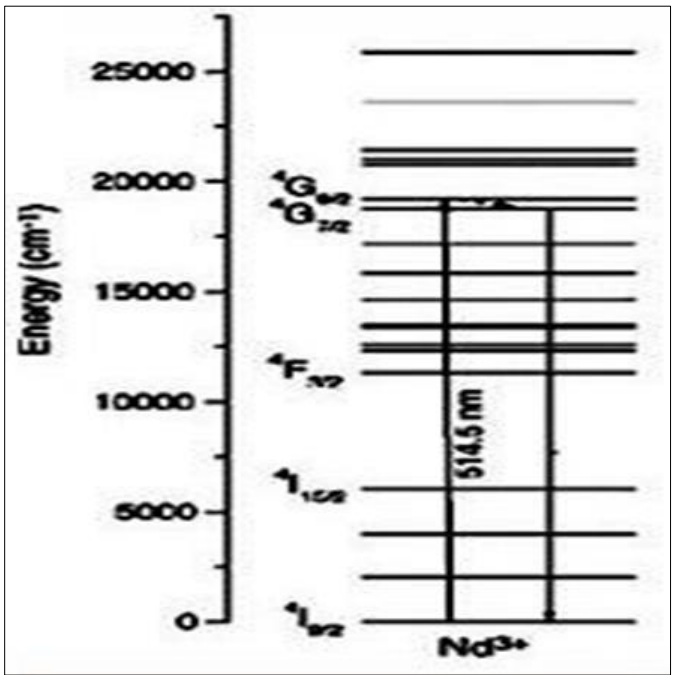

Fig 5: Schematic energy level diagram of Nd^{3+}

3.6 Sm^{3+}

Sm^{3+} works as an auxiliary activator in photo-stimulable SrS: Sm^{3+} phosphor, giving the transitions at 600 nm (^{4}G5/2 - ^{4}H7/2 and 646 nm (^{4}G5/2- ^{6}H9/2), [54] when utilized as activators.

The greatest emission in the nanocrystalline YAlO3:Sm^{3+} materials investigated by Isha Gupta *et al*. is seen at 604 nm due to the ^{4}G5/2- ^{6}H7/2transition, in the reddish-orange emission. The ^{6}H5/2 - ^{6}P3/2 intraconfigurational f-f transition was the source of the excitation at 405 nm, making Sm3+phosphor an effective material for powered LED applications. This material was successfully synthesized using the solution combustion (SC) synthetic technique at 1055 nm [55].

An innovative Ba2GdV3O11 nanophosphor series doped with trivalent samarium emits white light as a result of stimulation at 324 nm, according to research by Priya Phogat *et al*. An alternative white light emitting material for WLEDs and lighting technology is Sm^{3+} doped Ba2GdV3O11 [56].

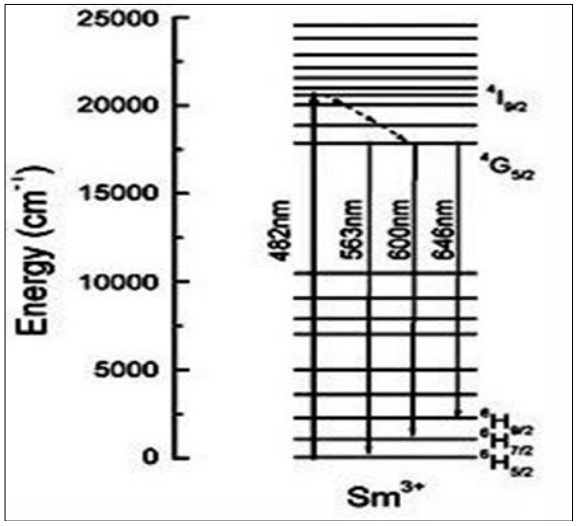

Fig 6: Energy level diagram of Sm^{3+}

3.7 Sm^{2+}

Due to (^{5}D0- ^{7}F0-4), these ions produce a transition from 550 to 850 nm. BaFCl: Sm^{2+} [49] phosphor is an instance of this kind, where Sm^{2+} serves as an activator. LiSrB9O15:Sm sample exhibits peaks in the 680–780 nm region that are associated with the transition of Sm^{2+} under 401 nm excitation [57]. Synthesis of SrB4O7:Sm^{2+} phosphor using the traditional solid-state process. Phosphors that have been doped with Sm^{2+} may one day be used in LED applications. The phosphor could be efficiently stimulated by UV-vis light between 250 and 500 nm, according to luminescence characteristics, and it displayed deep red (685 nm) emission [58] associated with the ^{5}D0 - ^{7}F0 transition of Sm^{2+} [59].

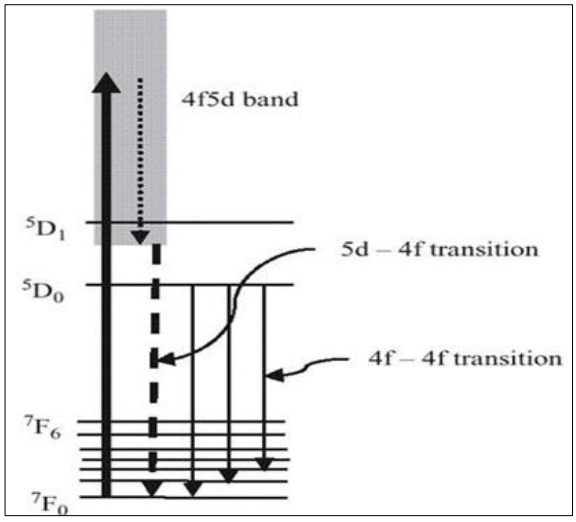

Fig 7: Energy level diagram of Sm^{2+} [61].

3.8 Eu^{2+}

Eu^{2+} ion luminescence in diverse hosts has attracted a lot of research because of its peculiar properties. Its excitation and emission spectra are typically broadband because of the difference in the crystal field components between the 4f6 5d excited state and the $^4f_7$ ($^8S_{7/2}$) ground state. Eu^{2+} emission is caused by two different kinds of transitions [29]. The most frequent is that which results from $^4f_6$ 5d- ($^8S_{7/2}$) [60].

Because the host has a significant impact on where the band that corresponds to the $^4f_6$ 5d configuration is located, the emission can range from 365 nm (for example, in $BaSO_4$) to 650 nm (for example, in CaS) [35], from the near UV to the red part of the visible spectrum [51]. This reliance is thought to be caused by the 5d level splitting in crystal fields [61]. The emission increases with the strength of the crystal field [62]. Sharp line luminescence caused by the f-f transition at 360 nm. $BaMgAl_{10}O_{17}:Eu^{2+}$ and $Ba_7F_{12}Cl_2:Eu^{2+}$ are two phosphors utilized in three-band fluorescent lamps that exhibit blue luminescence, respectively [63].

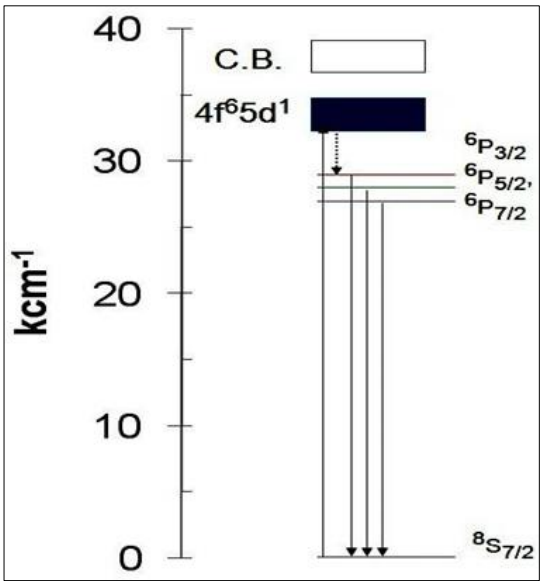

Fig 8: Energy level diagram of Eu^{2+}

3.9 Gd^{3+}

Gd^{3+} phosphors emit light in the UV spectrum. The Gd^{3+} (^{6}P7/2 longest)'s excited it level produces crisp line luminescence at a wavelength of 315 nm [64] and sensitizes other rare-earth ions' luminescence more [65]. Due to the greatest rare-earth ions' energies and the charge transfer spectra's energy level, Gd^{3+} doesn't induce other rare-earth ions to quench.

The major UVB emissions of the Gd^{3+} doped phosphor (LaPO4) stimulated at 272 nm correlate to the ^{6}P7/2- ^{8}S7/2 transitions of Gd^{3+} generated by the co-precipitation process at different concentrations of Gd^{3+} at 312 nm in the photoluminescence (PL) emission spectra [66].

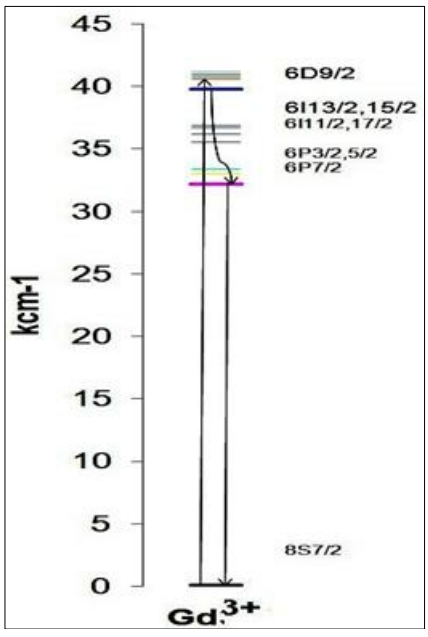

Fig 9: Energy level diagram of Gd^{3+}

3.10 Tb^{3+}

Lines resulting from $^5D4$- ^7FJ are present in the luminescence spectra of Tb^{3+}, but the $^5D4$- $^7F5$ emission line, which is present in almost all host crystals, is the brightest of these lines at about 550 nm [67]. Examples of Tb^{3+} activator phosphors include Ln2O2S:Tb^{3+} and SrAl4O7:Tb^{3+}. These samples were made using the sol gel combustion method, and they showed yellowish-green emission with the highest peak at 520 nm due to the $^5D4$- $^7F5$ transition, despite the fact that the PL of SrAl2O4:Tb^{3+} showed characteristic emissions at 488, 543, On the other hand, SrAl2O4:Tb^{3+} had a broad spectrum with a peak that was centered at about 520 nm [68-69].

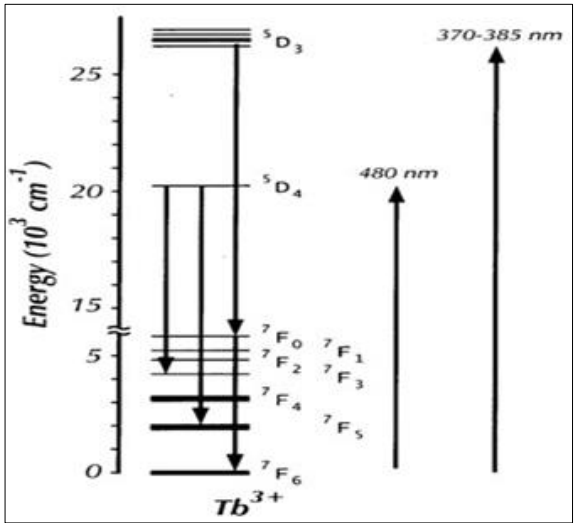

Fig 10: Schematic energy level diagram of Tb^{3+}

3.11 Er^{3+}

As a result of Er^{3+} 's $^4S3/2$ to $^4I15/2$ transition in infrared to visible up-conversion phosphors, it has been noted that Er^{3+} doped phosphors display green light [70]. Examples of Er^{3+} activators include Y2O3:Er^{3+} and Y2O3S:Er^{3+} [71].

Significant absorption peaks are visible in the UV-Vis spectra of zinc-lead-phosphate glass at wavelengths of 1536, 979, 799, 650, 523, and 485 nm. Peaks in the emission are seen at 502, 545, and 606 nm, respectively. The use of phosphors that have been doped with Er^{3+} may be advantageous for the creation of solid state lasers and other photonic devices [72].

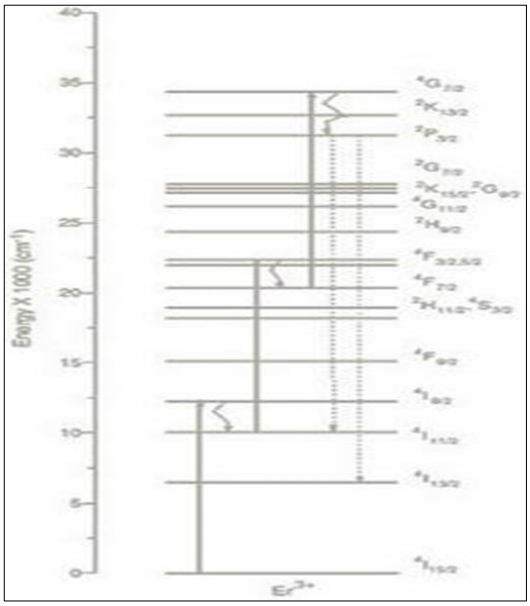

Fig 11: Energy level diagram of Er^{3+}

3.12 Tm^{3+}

The ($^1G_4$-$^4H_6$) transition has been observed in infrared to visible up-conversion phosphors, and this transition is what causes the blue light of Tm^{3+} to be detected.

The PL spectral properties of potassium zinc aluminium borosilicate (KZABS) glasses doped with Tm^{3+} ions exhibit blue and red colours at different excitation wavelengths. The absorption spectra in the UV-Vis-NIR range demonstrate the significant band gap energy [73].

The glasses exhibit PL emission in the blue and red regions, respectively, at excitation wavelengths of 359 and 466 nm [74].

For use in blue/red-emitting photonic devices, such as w-LEDs, phosphors can be employed as Tm^{3+} doped KZABS glasses. ZnS doped with Tm^{3+} [75] is the best illustration of Tm^{3+} when it is utilised as an activator [73].

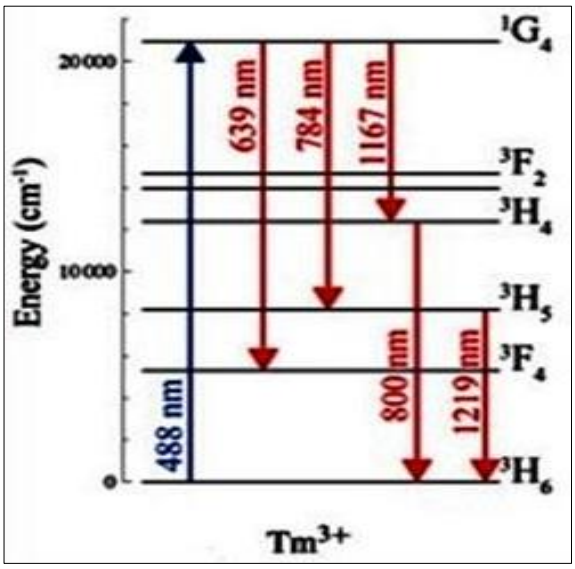

Fig 12: Energy level diagram of Tm^{3+}

3.13 Yb^{3+}

Yb^{3+} shows $^4F5/2$ - $^5F7/2$ transition, the Yb^{3+} absorbs infrared light at 1000 nm. La2O2S:Yb^{3+} and ZrO2 Nano phosphor, which were produced using the combustion synthesis method (CSM) and stimulated by a 980 nm laser with a changeable ytterbium concentration, are examples of Yb^{3+} acting as an activator. The PL emission spectrum displays strong emission peaks at 987, 998, and 1021 nm, all of which are in the infrared spectrum [76].

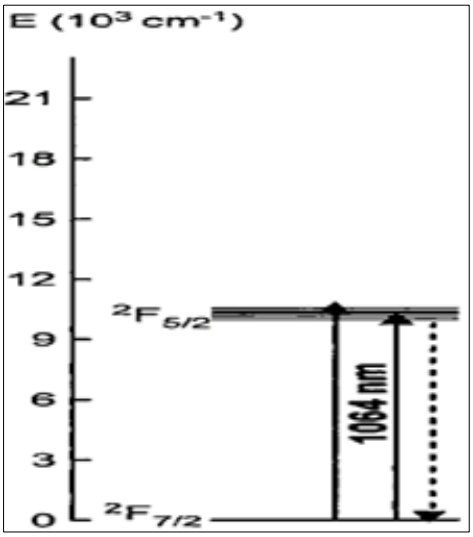

Fig 13: Energy level diagram of Yb^{3+}

3.14 Ho^{3+}

RE^{3+} ion Ho^{3+} can be ionized by infrared and visible light lasers. Shows emission due to transition from (^{5}Fi (i=3,4,5) - ^{5}I8) and (^{5}S2 - ^{5}I7) for Ho^{3+} ion by absorption [77].

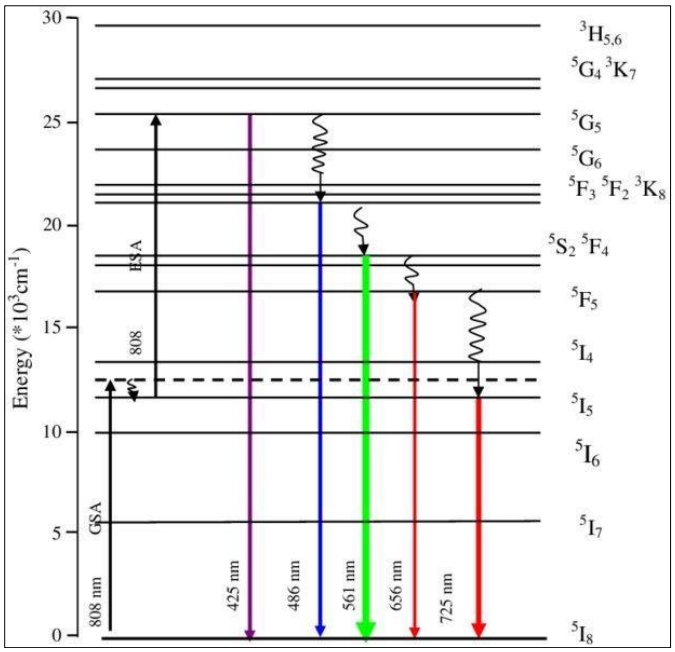

Fig 14: Schematic energy level diagram of HO^{3+}

4. Photoluminescence emission in transition metal

Transition metal ions' electron configuration is d^n (0< n <10), meaning that their d-shell is not completely filled. Tanabe and Sugano estimated the energy levels resulting from such a structure while accounting for the mutual interaction between the crystal field and the d-electron. A transition metal (TM) impurity causes physicochemical characteristics that are not present in the pure host lattice of an insulating material to manifest. These characteristics may be advantageous for practical devices such as storing phosphors and solid-state lasers, among others. Despite the fact that a doped material is undoubtedly more complex than an uncontaminated one [78].

4.1 Mn^{2+}

The well-known representative of luminous materials is Mn^{2+}. The Mn^{2+} ion actually has an almost colorless spectrum. Yet, Mn^{2+} compounds with a bright rose colour, such as MnF2 and MnCl2. The emergence of physicochemical properties that are not present in the pure host lattice as a result of the presence of a transition metal (TM) impurity in an insulating material may be helpful for applied devices like solid-state lasers and storage phosphors, among others [79]. The two kinds of Mn^{2+} activated phosphors that emit green and orange-to-red light, respectively, are generally recognized [79-80]. The latter class includes ZnGa2O4: Mn^{2+} as a well-known example [81]. Selecting a lattice with Mn^{2+} at a place that is considerably farther from the Mn^{2+} radius is another method for getting a green Mn^{2+} emission. SrB6O10: Mn^{2+}, whose Mn^{2+} emission is observable at 512 nm, [82] is one example of a molecule that meets this requirement [83].

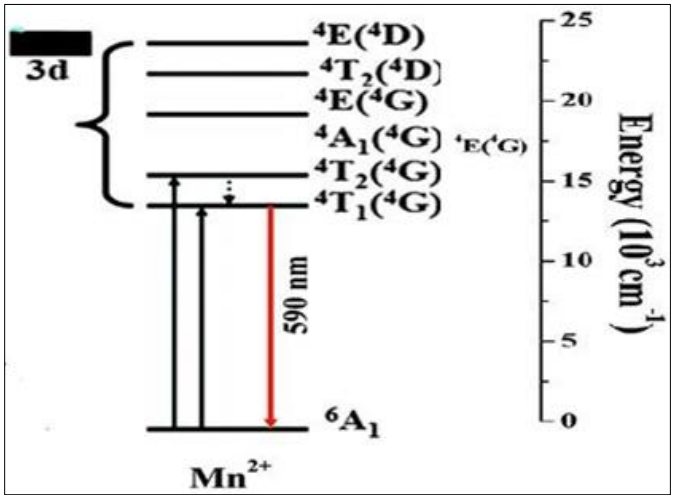

Fig 15: Schematic energy level diagram of Mn^{2+}

4.2 Cu^+

At normal temperature, Cu^+ ions exhibit monovalent d^{10} emission that is frequently effective. Cu^+ ion has a $3d^{10}$ ground state electrical arrangement. By definition, fluorescence mechanisms should involve 3dl0 - 3d94s transitions, which are totally forbidden for free ions but are somewhat permitted in crystals or glasses via coupling with odd parity lattice vibrations. Hence, the excitation and emission bands are fairly wide [84].

Moreover, significant spectrum distribution modulations that are consistent with the characteristics of the material are brought on by the Stoke's shift and excited state energies, which are likewise significantly reliant on the size and symmetry of the copper site. The emission quantum yield of monovalent copper in oxygenated insulators, which is a distinct perspective, can be rather high under certain conditions [84]. This can be demonstrated by contrasting the distinct emissions of two materials often used in fluorescent lamps-a ground copper activated borate glass and an N.B.S. classical standard-under the same 254 nm continuous excitation. A luminescence quantum yield of this glass is around 50% [84].

Devices with full-color electroluminescent displays can also use Cu^+ emission as their blue component. Copper's more prevalent valency is 2^+, but methods for incorporating monovalent Cu have not been systematically developed [85]. For instance, results on Cu^+ emission in alkali halides have been mentioned in several works [31, 86], but the method used for incorporating Cu in monovalent form has not been provided.

The states involved in the luminescence process are shown in figure along with the probabilities of transition for Cu^+ ions [3]. The system is first stimulated from the ground state ($3d^{10}$ configurations) to the singlet state of the $3d^94s_1$ configuration, after which the electrons proceed to the triplet state, mostly to level 2 due to symmetry considerations [38]. A free Cu^+ ion's ground state has the structure $3d^{10}$. While the transitions from $3d^{10}$ to $3d^94s$ and $3d^{10}$ to $3d^94p$ fill the lowest enthusiastic states. As a result, the singlet state has no impact on the luminescent process because the final transition occurs so

quickly compared to the other steps that it may be said to be instantaneous. The two energy levels of the triplet state, 2 and 3, are capable of non-radiative transitions with probabilities of p23 (from level 2 to level 3) and p32 (from level 3 to level 2). With probabilities A21 and A31, respectively, radiation from levels 2 and 3 transitions to the ground state (level 1) [38]. The strong coupling scheme is indicated by the stoke's shift of the Cu^{+} emission, which is often substantial (>5000 cm^{-1}).

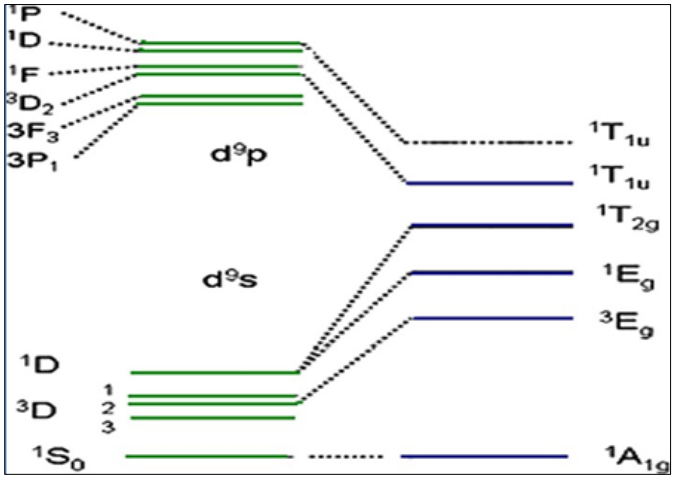

Fig 16: Energy level diagram showing the states involved in the luminescence process and the transition probabilities in Cu^{2+}

4.3 Cr^{3+}

Emission is in the deep red area (emission two sharp lines called R- lines). Emission typically ranges from ^{2}E to $^{4}A_2$. The lowest excited state is where transition metal ions are first released. The $^{4}T_2$ level is lower for crystal fields that are not very high, making the ^{2}E level not always the lowest excited state. In that situation, the emission has a decay period of 100 us and is in the infrared broad band $^{4}T_2$ - $^{4}A_2$. At 4.2 K, $YAl_3B_4O_{12}$'s Cr^{3+} emission is ^{2}E- $^{4}A_2$, whereas at higher temperatures, it is $^{4}T_2$ - $^{4}A_2$. [87].

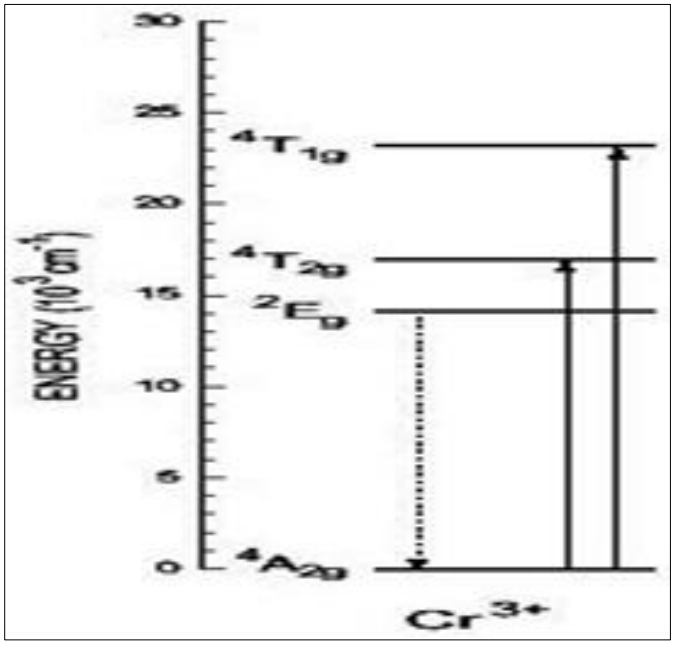

Fig 17: Energy level diagram of Cr^{3+}

5. Conclusion

The introduction to this chapter included the specifics of lanthanides as well as the transition metal ions. We describe in detail the spectroscopic transitions, energy level structure, and processes in a wide range of lanthanide ions and transition metal ions. Generally, the introduction of the lanthanide ions' fundamentals in this chapter is done nicely.

6. References

1. Vij DR. Luminescence of solids Plenum Press New York, USA. 1998;131:361-386
2. Harvey EN. A History of Luminescence from the earliest times until. 1900-1957;44:692.
3. Kartik N Shinde, Dhoble SJ, Swart HC. Kyeongsoon Park. Phosphate Phosphors forSolid-State Lighting 174, Springer Science and Business Media LLC; c2012.
4. Welker T. Journal of Luminescence; c1991. p. 48-49, 49-56.
5. Blasse G, Bril A, Philips Tech. Rev. 1970;31:303.
6. Eliseeva SV, Bunzli J. Chem. Soc. Rev. 2010;39:189.
7. Xia Z, Liu Q. Prog. Mater. Sci. 2016;84:59-117.
8. Ye S, Xiao F, Pan YX, Ma YY, Zhang QY. Materials Science and Engineering: R: Reports; c2010. p. 71.
9. Xiaopeng Fu, Wei Lü, Mengmeng Jiao, Hongpeng, Inorganic Chemistry, 2016, 55(12).
10. Pires A, Davolos MR. Chem. Mater. 2001;13:21.
11. Ch I, Chen TM, Chen J. Mater. Res. 2001;16:644.
12. Lin YH, Zhang ZT, Tang ZL, Zhang JY, Zheng ZS, Lu X. Mater. Chem. Phys. 2001;70:156.
13. Jia W, Yuan H, Lu L, Liu H, Yen WM, Lumin J. 1998;76/77:428.
14. Jia D, Zhu J, Wu B, Lumin J. 2001;93:107.
15. Ping Yang, Meng Kai Lü, Dong Xu, Duo Rong Yuan, Chun Feng Song, Zhi Qiang Liu, *et al*. Materials Science and Engineering: B. 2002;96:33-36.
16. Chang Chengkang, Li Wen, Huang Xiaojun, Wang Zhiyu, Chen Xi, Qian Xi, *et al*. Journal of Luminescence, ISSN:0022-2313, 130 (2010-03)3, 347-350.
17. Vijay B Pawade, Vibha Chopra, Dhoble SJ. Introduction to electronic spectroscopy of lanthanide, properties, and their applications, Elsevier BV; c2020
18. Tanaka K, Suzuki S, Choo CK. J Appl. Phys. 2004;95:1294.
19. Tanaka K, Miyajima T, Shirai N, Zhuang Q, Nakata R. J Appl. Phys. 1995;77:6581.
20. Pustovarov A, Krymov AL, Shulgin BV, Zinin EI. Rev. Sci. Instrument. 1992;63:3521.
21. Nikolaenko TN, Hizhnyi YA, Nedilko SG. J Lumin. 2008;128:807.
22. Gedam SC, Dhoble SJ, Moharil SV. Journal of Luminescence. 2008;128(1):1-6.
23. Philips Res. Rep. 1952;7:1-20
24. Morgan GP, Yen WM. Topics in Appl. Phys. Springer. 1989;77(122):65.
25. Ishwar Prasad Sahu. Journal of Materials Science: Materials in Electronics, 2017, 28(1). DOI: 10.1007/s10854-016-5534-x
26. Ingole DK, Joshi CP, Moharil SV, Muthal PL, Dhopte SM. 2011;131(12):2499-2502
27. Talwar GJ, Joshi CP, Moharil SV, Dhopte SM, Muthal PL. Kondawar VK. Journal of Alloys and Compounds. 2011;509(35):8742-8747.
28. Nita Shinde, Dhoble NS, Gedam SC, Dhoble SJ. Journal of Luminescence. 2016;172:131-138.
29. Kore, Bhushan P, Dhoble NS, Lochab SP, Dhoble SJ. Journal of Luminescence. 2014;145:299-306.
30. Sahu AK, Bhushan P Kore, Chowdhary PS, Nayar V, Dhoble SJ. 2014, 29(1). 10.1002/bio.2502

31. Sharadkumar C Gedam, Sanjay J Dhoble. Journal of Luminescence. 2012;132(10):2670-2677
32. Blasse G. Energy Transfer Process in Cond. Mat., Ed- B. DiBartolo, Plenum Press, N.Y., 1983, 251.
33. Phy ZJ. Kiss, Phys. Rev. 1962;1277:718.
34. Dorenbos P, *et al*., Nucl. Instrum. Methods Phys. Res. B. 1998;134:304.
35. Kongre VC, Gedam SC, Dhoble SJ. Journal of biological and chemical luminescence; c2015.
36. Blasse G, Brill A. J Chem. Phys. 1967;47:5139.
37. Blasse G, Brill A, J Chem. Phys. 1969;51:3252.
38. Sharadkumar C Gedam, Sanjay J Dhoble. J Lum. 2012;132(10):2670.
39. Poddar, Anuradha SC Gedam, Dhoble SJ. Lum. 2013;143:579-582.
40. Taikar DR, Joshi CP, Moharil SV. Luminescence. 2017;32(6):902-907
41. Lucimara C Bandeira, Katia J Ciuffi, Paulo S Calefi. Eduardo J. Nassar. 2010;1:200-207.
42. Sanjay J Dhoble, Lehlohonolo Koao, Vijay Pawade, Atul N. Yerpude Elsevier BV; c2023.
43. Su Q, Pei Z, Chi L, Zhang H, Zhang Z, Zou F, J Alloy. Comp. 1993;192:25.
44. Van Uitert LG, Soden RR. J Chem. Phys. 1962;36:517.
45. Shoaib MM, Khan I, Rooh G, Wabaidur SM, Islam MA, Chanthima N, *et al*. J. Lum. 2022;247:118884.
46. Meiling Liu, Lianhua Tian, Optik. 2021;242:166866.
47. Gaft M, Raichlin Y. Physics and Chemistry of Minerals, 2020, 47(1).
48. Annadurai G, Masilla S. Moses Kennedy, Sivakumar V. Superlattices and Microstructures. 2016;93:57-66.
49. Watanabe M, Nishimura T, Kohmoto K, Tech DP. Res. Soc. meeting Luminescence: Phenomena, Applications and Materials; c1977.
50. Kato A, Oishi S, Shishido T, Yamazaki M, Iida S. Journal of Physics and Chemistry of Solids. 2005;66(11):2079-2081
51. Devender Singh, Vijeta Tanwar, Shri Bhagwan, Ishwar Singh. Recent Advancements in Luminescent Materials and Their Potential Applications, Wiley; c2016.
52. Padlyak BV, Lisiecki R, Padlyak TB, Adamiv VT. Journal of Luminescence. 2018;198:183-192
53. Samar Jana, Subrata Mitra. Optics & Laser Technology. 2021;141:107123.
54. Kaczmarek SM, Leniec G, Berkowski M, Kazan S, Açıkgöz M. Journal of Alloys and Compounds. 2016;687:(5):696-700.
55. Isha Gupta, Sitender Singh. Journal of Molecular Structure. 2022;1267:133567.
56. Priya Phogat, Taxak VB, Khatkar SP, Malik RK. Chemical Physics. 2022;561:111623.
57. Pu Fan, Zongjie He, Yuhui Chen, Xiao He, Cong Huang, Qiqi Miao, *et al*. Journal of Luminescence. 2022;251:119169.
58. Zhongmin Cao, Xiantao Wei, Lu Zhao, Yonghu Chen, Min Yin. ACS, Applied Materials & Interfaces. 2016;850:34546-34551.
59. Jiayue SUN, Jicheng ZHU, Xiaotang LIU, Haiyan DU. Journal of Rare Earths. 2012;30(11):1084-1087.
60. Blasse G, Wanmaker WL, Tervrugt IW. Phi. Res. Rept. 1968;23:189.
61. Verstegen JMPJ, Radielovic Dk, Vrenken LE. J Electrochern. Soc. 1974;121:1627.
62. Takesue M. Journal Progress in Crystal Growth and Characterization of Materials. 2009;55(3-4):98-124.
63. Caroline Hasler. Andreas Hauser Jacob Olchowka Hans Hagemann J of Lum. 2021;233:117866.
64. Sommerdijk JL, Stevels A. Philips Tech. Rev. 1977;37:221.
65. Stevels A, Verstegen J, Lumin J. 1976;14:207.
66. Vijay Singh B, Rupa Venkateswara Rao, Rao AS, Rao JL. Muhammad Irfan, Optik. 2020;206:164020.
67. Apple EF, Ishler WE. Proc. Int. Conf. Lumin. of Organic and Inorganic Materials, N. Y. 1962, 576.
68. Bao-gai Zhai, Hanfei Xu, Qing Zhang, Yuan Ming Huang, ACS Omega. 2021;6(15):10129-10140.
69. Zhai BG, Huang YM. J Mater Sci. 2017;52:1813-1822.
70. François Auzel. Chem. Rev. 2004;104(1):139-174.
71. Bloch S, Burley G, Perlof A, Mason RD. J Res. NBS. 1959;62:95.
72. Haydar Aboud, Raja J Amjad. Journal of Non-Crystalline Solids. 2017;471:1-5.
73. Ravita AS. Rao, Journal of Non- Crystalline Solids. 2022;585:121532.
74. Dwivedi Y. Optical Materials. 2009;31(10):1472-1477.
75. De Hair J, Van Kemenade TC. Sci. and Techn of Light, Toulouse; c1983.
76. Raunak Kumar Tamrakar, Neha Tiwari, Vikas Dubey. Kanchan Upadhyay Journal of Radiation Research and Applied Sciences. 2019;145(3):399-403.
77. Vijay B Pawade, Vibha Chopra, Dhoble SJ. Introduction to electronic spectroscopy of lanthanide, properties, and their applications, Spectroscopy of Lanthanide-Doped Oxide Materials; c2020.
78. Barriuso MT, Moreno M, Aramburu JA. Physical Review B. 2002;65(6):064441.
79. Sommerdijk JL, Brill A, Hoex-Strik FMJH. Philip. Res. Rept. 1977;32:119.
80. Su Quing, Pei Z, Lin J, Xue F. J Alloy Comp. 1995;225:103.
81. Blasse G, Grabmaier BC. Luminescent Materials. Springre-Verlag, Berlin; 1994.
82. Shinde KN, Nagpure IM, Abhay B Fulke, Dhoble SJ. Luminescence. 2011;26(5):363-367
83. Poort SHM, Meijerink A, Blasse G. Solid State Commu. 2000;103:537.
84. Parent C, Boutinaud P, Le Flem G, Moine B, Pedrini C, Garcia D, Faucher M. Optical Materials. 1994;4(1):107-113.
85. Puppalwar SP, Dhoble SJ. Animesh Kumar, Luminescence, Luminescence. 2011;26(6):456-61.
86. Fussgaenger K. Phys. Status Solidi. 1969;34:157.
87. Kellendonk F, Belt T. van den, Blasse, Journal of Chemical Physics; c1982.